Quantification of *Plasmodium falciparum* Cyclophilin 19B Transcripts Via qPCR in Normal and Sickle-Trait Hemoglobin Genotypes

by

Natalie Vance

Duke Global Health Institute
Duke University

Date:_____

Approved:

_____
Steve Taylor, Advisor

_____
Joseph Egger

_____
Emily Derbyshire

Thesis submitted in partial fulfillment of
the requirements for the degree of
Master of Science in the Duke Global Health Institute
in the Graduate School of Duke University

2021

ABSTRACT

Quantification of *Plasmodium falciparum* Cyclophilin 19B Transcripts Via qPCR in Normal and Sickle-Trait Hemoglobin Genotypes
by

Natalie Vance

Duke Global Health Institute
Duke University

Date:_____
Approved:

_____
Steve Taylor, Advisor

_____
Joseph Egger

_____
Emily Derbyshire

An abstract of a thesis submitted in partial
fulfillment of the requirements for the degree
of Master of Science in the Duke Global Health Institute
in the Graduate School of Duke University

2021

Abstract

The sickle-cell trait hemoglobin genotype (HbAS) is known to protect against severe malaria caused by *Plasmodium falciparum.* However, the biological mechanisms behind this protection are not well understood. Cyclophilin 19B (*Pf*CyP-19B) is a parasitic gene that produces the protein cyclophilin 19B, a member of the unfolded protein response that is important in parasitic protein folding and trafficking. We set out to measure the transcript expression level of *Pf*CyP-19B to investigate its potential role in the mechanisms that confer protection for HbAS individuals. RNA was extracted from both *in vivo* samples collected from Malian children as well as *in vitro* samples harvested throughout a 48-hour incubation period. RNA extracts were reverse transcribed and transcript expression was measured via qPCR. Wilcoxon rank sum and bootstrapping methods were used to analyze transcript units between parasites grown in normal (HbAA) and HbAS red blood cells. The results from our cross-sectional *in vivo* data revealed a reduction in expression of *Pf*CyP-19B among individuals with the HbAS genotype compared to those with the HbAA genotype (Wilcoxon rank sum p=0.006). *In vitro* time series results showed no significant difference in *Pf*CyP-19B transcript expression levels between genotypes but did display a 24-hour pattern of peak expression for both HbAA and HbAS genotypes. The under expression of *Pf*CyP-19B among HbAS individuals could be linked to impaired protein trafficking, interfering with the parasite's ability to display surface proteins vital for cytoadherence and severe

disease manifestation. The 24-hour peak transcript expression displayed *in vitro* roughly aligns with the *P. falciparum* parasite stage transition states, suggesting cyclophilin 19B may aid in parasitic transitions.

Dedication

For my grandmother, Margaret: without your support this experience, and all that I have learned from it, would not have been possible.

Contents

List of Tables

List of Figures

Acknowledgements

I would like to acknowledge Steve Taylor and all members of the Taylor lab for welcoming me into their group under unexpected circumstances. I would like to personally thank Jens Petersen, Joseph Saelens, and Betsy Freedman for their guidance and assistance in the lab. Additionally, I would like to thank Christine Markwalter, Thynn Thane, Tim Veldman, and Joyce Hogue for their unwavering support as we all made some difficult transitions. I would particularly like to thank Zay Yar Han, an outstanding classmate, lab mate, roommate, and friend, for always maintaining a positive outlook and keeping things light-hearted. Thank you to my committee members, Steve Taylor, Joseph Egger, and Emily Derbyshire for their expertise and guidance throughout the thesis planning and writing processes. I would like to acknowledge the Malian children who participated in the clinical trial and whose blood samples were used in this study, as well as our partner members who were involved in all parts of the study. Additionally, thank you to the blood donors at Duke University for their contribution to our *in vitro* experiments. Thank you to the Duke Global Health Institute and the education team for their flexibility and support throughout the COVID-19 pandemic. Thank you to my classmates, friends, and family for encouraging and motivating me throughout this endeavor. This study was supported by a grant from the International Centers of Excellence for Malaria Research (ICEMR) and the Duke University Dean's Research Award.

1. Introduction

1.1 Malaria

Malaria is a deadly parasitic disease transmitted by female *Anopheles* mosquitoes. Although the parasite has likely been around since Neolithic times, it was not discovered as a protozoan parasite and identified with the genus *Plasmodium* until 1880.[1] Several years later, in 1897, the disease vector was identified as female *Anopheles* mosquitoes.[1] Malaria has plagued human populations for centuries, and while there have been improvements in diagnostic, treatment, and prevention methods, the disease is still responsible for nearly 400,000 deaths annually, most of which are children under the age of five.[2] Five different species of *Plasmodium* have been identified as capable of infecting human hosts: *P. falciparum, P. vivax, P. ovale, P. malariae,* and *P. knowlesi*. Most cases and deaths worldwide are attributed to *P. falciparum* and *P. vivax,* but in the malaria endemic regions of Africa, *P. falciparum* comprises the majority of the caseload.

The *Plasmodium* life cycle is complex with numerous stages in both human and mosquito hosts (Figure 1). Malaria is transmitted to humans via a bite from an infected female *Anopheles* mosquito. When the mosquito takes a blood meal, parasitic sporozoites are injected into the bloodstream of the human. During the exo-erythrocytic cycle, sporozoites travel to the liver where they infect hepatocytes and rapidly multiply, producing tens of thousands of merozoites per sporozoite forming a schizont.[3] This rapid multiplication causes the schizont to burst, releasing merozoites back into the

bloodstream where they infect red blood cells (RBCs) and enter the erythrocytic cycle. Once in the RBC, the merozoite matures to a trophozoite, again forming a schizont that ruptures, and continues the erythrocytic cycle. This cycle, also known as the asexual cycle, occurs roughly every 48 hours for *P. falciparum* and *P. vivax* and is responsible for the classic cyclical fever that is seen in clinical malaria cases. Various host and environmental factors can cause a portion of the asexual parasites to commit to gametocytogenesis, the sexual cycle. A sexually committed schizont releases merozoites that mature into either male microgametes or female macrogametes. These gametocytes undergo a series of developmental stages, growing to eventually inhabit most of the erythrocyte they have infected (Figure 1). To perpetuate the *Plasmodium* life cycle, a mosquito must ingest both a mature male and female gametocyte. Once ingested, microgametes penetrate macrogametes to form a zygote that then develops into a motile ookinete capable of crossing the mosquito midgut. In the midgut, the ookinete develops into an oocyst where sporozoites are formed, eventually causing the oocyst to rupture. When the oocyst ruptures, infectious sporozoites are released and travel to the mosquito's salivary glands where they wait to be transmitted to a human host during a blood meal.

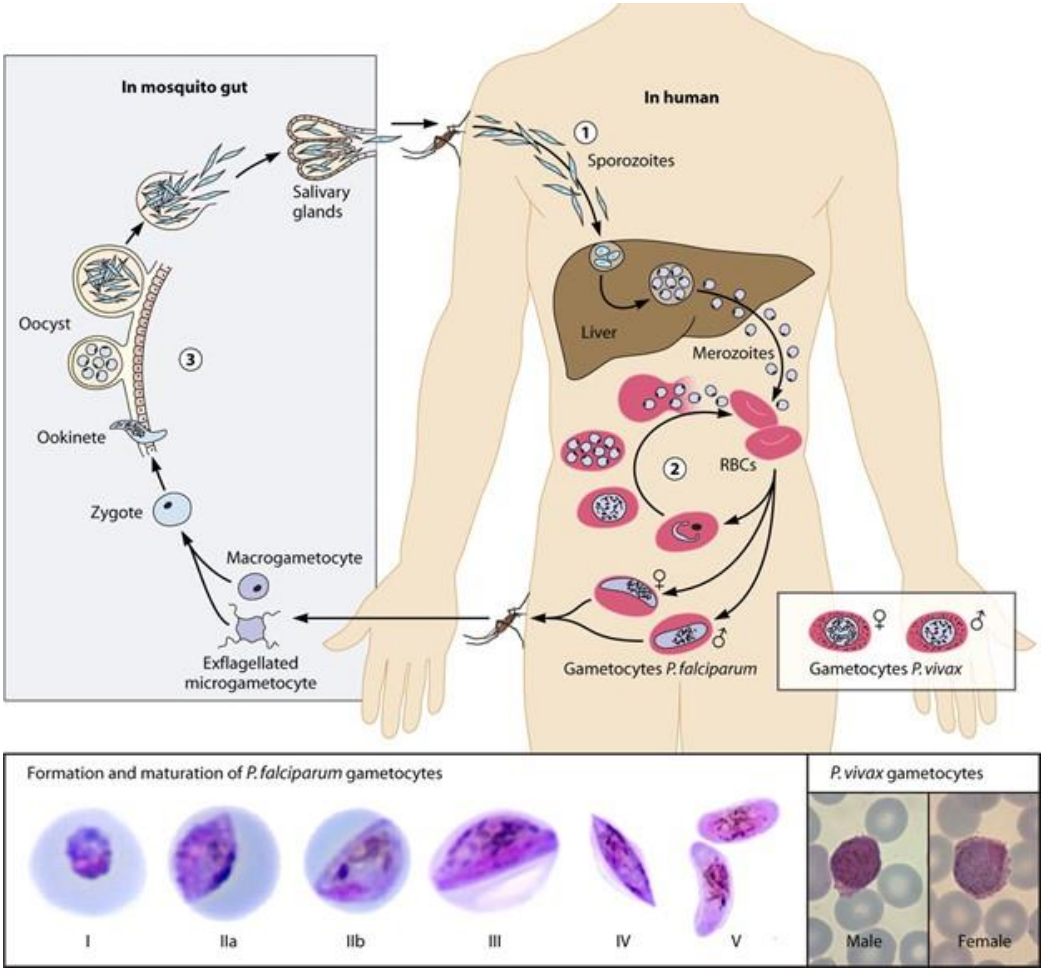

Figure 1: Malaria life cycle in the human and mosquito hosts. Bottom panel: developmental stages of *P. falciparum* gametocytes (left) and male and female *P. vivax* gametocytes (right). Figure reproduced with permission.[3]

Clinical disease presents many non-specific symptoms including headache, fatigue, fever, chills, and malaise. If left untreated, uncomplicated malaria can progress to severe malaria which can manifest with coma, metabolic acidosis, severe anemia, hypoglycemia, acute renal failure, or acute pulmonary edema.[4] In cases of severe *P. falciparum* malaria, infected RBCs bind to the endothelium (cytoadherence) or other infected and uninfected RBCs, forming erythrocytic aggregates known as rosettes which

can sequester in the microvasculature.[5] This sequestration can obstruct the microcirculatory pathways which in the brain can result in cerebral malaria. Severe malaria is often fatal. However, at the early stages of infection, uncomplicated malaria can be treated with proper medications, the most common of which for *P. falciparum* are artemisinin-based combination therapies (ACTs).

Although the causative agent of malaria was first discovered in 1880, historical findings suggest that the disease dates back to Neolithic times with evidence of a disease causing cyclical fever and splenomegaly persisting in various populations throughout time.[6] While malaria elimination is possible, and has been achieved in low-, middle-, and high-income countries like Sri Lanka, Paraguay, Algeria, the United States, and most recently El Salvador, the disease is still transmitted throughout much of the tropics (Figure 2). According to the World Health Organization (WHO), the African Region has the greatest malaria morbidity, accounting for 94% of the global burden.[2] Between 2000 and 2019, global malaria cases have decreased from 238 million to 229 million.[2] Likewise, global malaria deaths have reduced from 736,000 in 2000 to 409,000 in 2019.[2] While these are notable improvements, there are still nearly 400,000 annual malaria deaths, 67% of which are among children under the age of five, indicating an ever-present need for further research into treatment and prevention methods.[2]

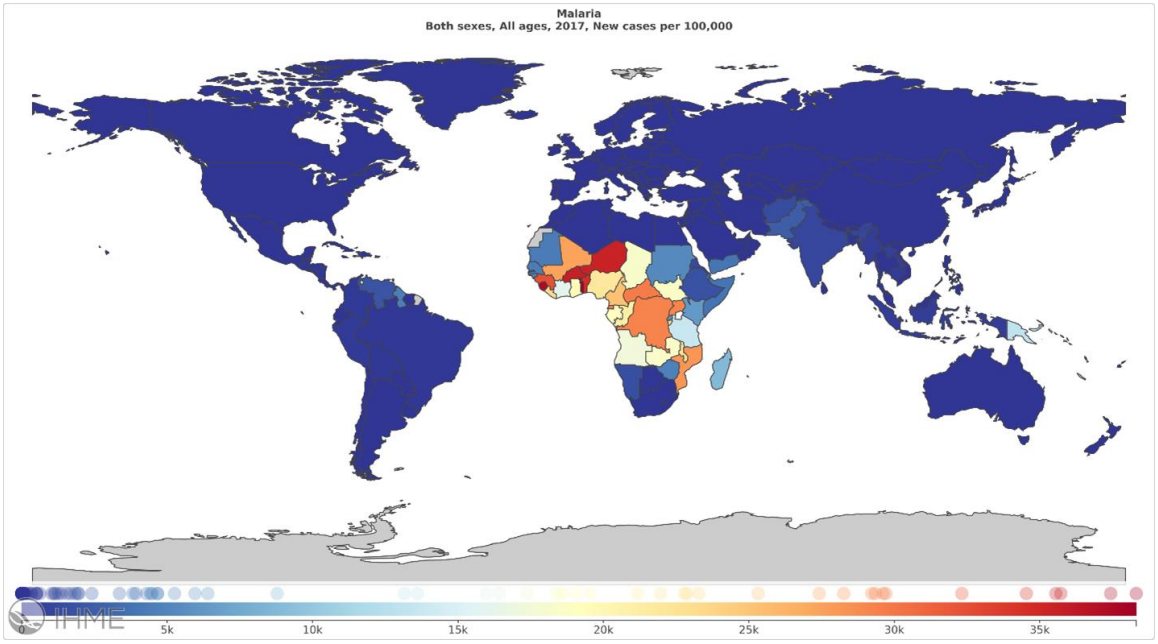

Figure 2: Worldwide malaria incidence as of 2017. Incidence measured in new cases per 100,000 population. Image generated from the Institute for Health Metrics and Evaluation (IHME) database.

1.2 Sickle-Cell Trait

Hemoglobin is a molecule found in red blood cells (RBCs) that facilitates the transportation of oxygen. Normal hemoglobin molecules have alpha and beta subunits (HbA;$\alpha_2\beta_2$). Sickle hemoglobin (HbS) is a variant of hemoglobin in which a single nucleotide polymorphism in the *HBB* gene causes a mutation (β^s) in the β globin subunit where the glutamic acid at the sixth position is replaced with the amino acid valine.[7] Sickle-cell anemia (SCA), the most common form of Sickle-cell disease (SCD) in Sub-Saharan Africa, is a hereditary disease that results from homozygous β^s alleles which cause RBCs to take on a sickle or crescent shape when they are deoxygenated.[8] SCA typically results in anemia, pain, dactylitis, frequent infections, and stroke. Without

expensive treatment options such as stem cell transplants, the prognosis for those diagnosed with SCA is poor.

There is an important distinction between the homozygous and heterozygous hemoglobin genotypes. While the homozygous genotype (HbSS) causes the disease sickle-cell anemia, the heterozygous genotype (HbAS), known as sickle-cell trait (SCT), is not disease-causing, but actually confers partial protection against severe *P. falciparum* malaria.[9] While the protective effects of HbAS were first observed in the mid-1940's,[10] it is still not fully understood how this protection is conferred on the molecular level and several mechanisms have been proposed. Studies from the 1970's showed evidence of increased sickling in parasitized HbAS RBCs compared to uninfected HbAS RBCs.[11,12] It was later hypothesized that this increased sickling could lead to increased phagocytosis of the infected RBCs (iRBCs) and thus lower levels of parasitemia in HbAS compared to HbAA.[13] Other studies found that *P. falciparum* ring-stage parasites experienced limited growth due to certain intra-erythrocytic conditions imposed by the HbAS genotype including the release of toxic ferriprotoporphyrin IX (FP) with increased denaturation of hemoglobin S,[14] and osmotic shrinkage of the RBC.[15] Results from an *in vitro* experiment supported the proposal that some human erythrocytic micro RNAs (miRNA) enriched in HbAS and HbSS erythrocytes can translocate into parasitic mRNA, resulting in reduced intra-erythrocytic growth.[16]

A more recently supported mechanism of protection suggests that HbAS iRBCs experience a reduction in cytoadherence. Cytoadherence is the process by which iRBCs attach themselves to endothelial cells in the microvasculature, this process is believed to be driven by the *P. falciparum* erythrocyte membrane protein 1 (PfEMP-1). Cytoadherence is an important mechanism in the formation of rosettes and also allows parasites to avoid clearance by the spleen.[17] HbAS iRBCs were found to have a reduced display of surface PfEMP-1 as well as decreased display of knobs (concentration points of PfEMP-1 on the erythrocytic surface) and abnormal knob morphology.[17,18] Additionally, one study found that HbAS impairs protein export to the surface of iRBCs, including that of PfEMP-1.[18] The combination of reduced cytoadherence and impaired protein export among HbAS iRBCs could inhibit their ability to sequester in the endothelial microvasculature, a key element to parasitic survival and severe disease manifestation. While there is evidence to support the aforementioned mechanisms of action, it is still not completely understood how the altered HbAS RBC environment confers protection against severe malaria.

1.3 Cyclophilin 19B

Cyclophilins, a member of the immunophilins, are ubiquitous in nature, existing in the cells of all prokaryotes and eukaryotes.[19] Many cyclophilins have peptidyl-prolyl isomerase (PPIase) activity that allows them to stabilize the *cis-trans* transition states of peptidyl-prolyl bonds and therefore speed up this rate-limiting isomerization step in

protein folding. While these proteins can have different functions depending on the organism in which they are transcribed, many are chaperones and due to their PPIase activity, play a key role in protein assembly in addition to protein folding.

In the *Plasmodium falciparum* genome, 11 cyclophilin or cyclophilin-like genes have been identified, though not all have been characterized functionally.[20] Cyclophilin 19B (*Pf*CyP-19B) is among those that have been characterized. Located in the cytosol of the parasite and most highly expressed in the schizont stage of the parasite life cycle, *Pf*CyP-19B is a peptidyl-prolyl isomerase and is therefore important in protein folding processes.[21] In addition to protein folding, *Pf*CyP-19B acts as a chaperone molecule, aiding in parasitic protein trafficking and regulation of multi-protein complexes.[21] Cyclosporines are known to bind to cyclophilins, and have been investigated as potential therapeutic targets. As such, *Pf*CyP-19B has been studied in the context of its binding properties with Cyclosporine A (CsA). CsA has shown chemotherapeutic capabilities as an antimalarial due to its ability to inhibit the PPIase activity of *Pf*CyP-19B when bound to the cyclophilin, resulting in slowed growth of the *P. falciparum* parasite.[21,22]

*Pf*CyP-19B has also been studied in the context of *P. falciparum* resistance to artemisinin, the leading pharmaceutical treatment of malaria. A human transcriptomics study in the Greater Mekong Subregion of Southeast Asia found *Pf*CyP-19B to be up-regulated in *P. falciparum* parasites exhibiting *Kelch-13* (K13) mutations characteristic of

artemisinin resistance.[23] The overexpression of *Pf*CyP-19B transcripts was correlated with other members of the unfolded protein response (UPR), a vital component in repairing the damage caused by artemisinin.[23]

In a comparative transcriptomics investigation of asexual stage *P. falciparum* parasites, our lab recently found that *Pf*CyP-19B was significantly downregulated in HbAS RBCs compared to HbAA RBCs both *in vitro* and *in vivo* (unpublished results). Along with other members of the *Plasmodium* reactive oxidative stress complex (PROSC) *Pf*CyP-19B was under expressed in HbAS *in vitro* at late time points in the intraerythrocytic development cycle. However, *in vivo*, *Pf*CyP-19B was the only member of PROSC that exhibited significant downregulation in HbAS RBCs. *Pf*CyP-19B has yet to be studied in depth in the context of the HbAS genotype, and such research may provide further insight into the mechanisms conferring protection as well as contribute to the functional understanding of *Pf*CyP-19B.

1.4 Research Question, Aims, and Hypothesis

The study objective was to explore the transcript expression levels of cyclophilin 19B among *P. falciparum* parasites grown in normal and sickle-cell trait red blood cells. Our first aim was to successfully measure *Pf*CyP-19B expression via quantitative polymerase chain reaction (qPCR) in two types of samples: *in vitro* time series samples from blood donors at Duke University Hospital and *in vivo* clinical samples from an observational study conducted in Mali. Our second aim was to determine if there is a

significant difference in *Pf*CyP-19B expression between *P. falciparum* parasites grown in normal and sickle-cell trait RBCs in both the *in vitro* samples and the Malian clinical samples. We hypothesized that *Pf*CyP-19B expression levels would be significantly lower in individuals with the sickle-cell trait genotype (HbAS) than in those with normal hemoglobin genotype (HbAA).

2. Methods

2.1 Setting

Mali is a malaria endemic country located in West Africa with diverse geography and a hot climate. Despite being among the largest countries in Africa, the population is relatively small, around 20 million.[24] The Sahara Desert stretches across northern Mali and into central Mali, while southern Mali is comprised of plateaus and plains with rich soil deposits along the Niger River. Temperatures are high (70^0F to 100^0F in southern and central Mali, 115^0F to 140^0F in the desert regions) year-round throughout the country, with the exception of the desert lands where temperatures can dip to 39^0F at night.[24] Malaria transmission is seasonal with intense transmission during the rainy season (June to October) and virtually none during the dry season (November to June). According to the WHO, in 2017 there were 1.9 million confirmed cases of malaria in Mali, much lower than the estimated caseload of 7.2 million (95% CI: 5.1 million to 10.2 million).[25] Similarly, the number of reported malaria deaths was much lower than the WHO's estimate, 1,050 and 12,400 (95% CI: 9,800 to 14,900) respectively.[25] As is the case worldwide, malaria poses a serious threat to Malian children, causing 14% of deaths in those under the age of five years.[26]

Clinical samples were collected from participants living in the agricultural village of Kenieroba (Figure 3). Samples were stored at the Malaria Research and Training Center in the nation's capital city of Bamako (Figure 3). All laboratory

procedures for this study were conducted in the Alex H. Sands Basic Sciences Research Building on Duke University's campus in Durham, North Carolina.

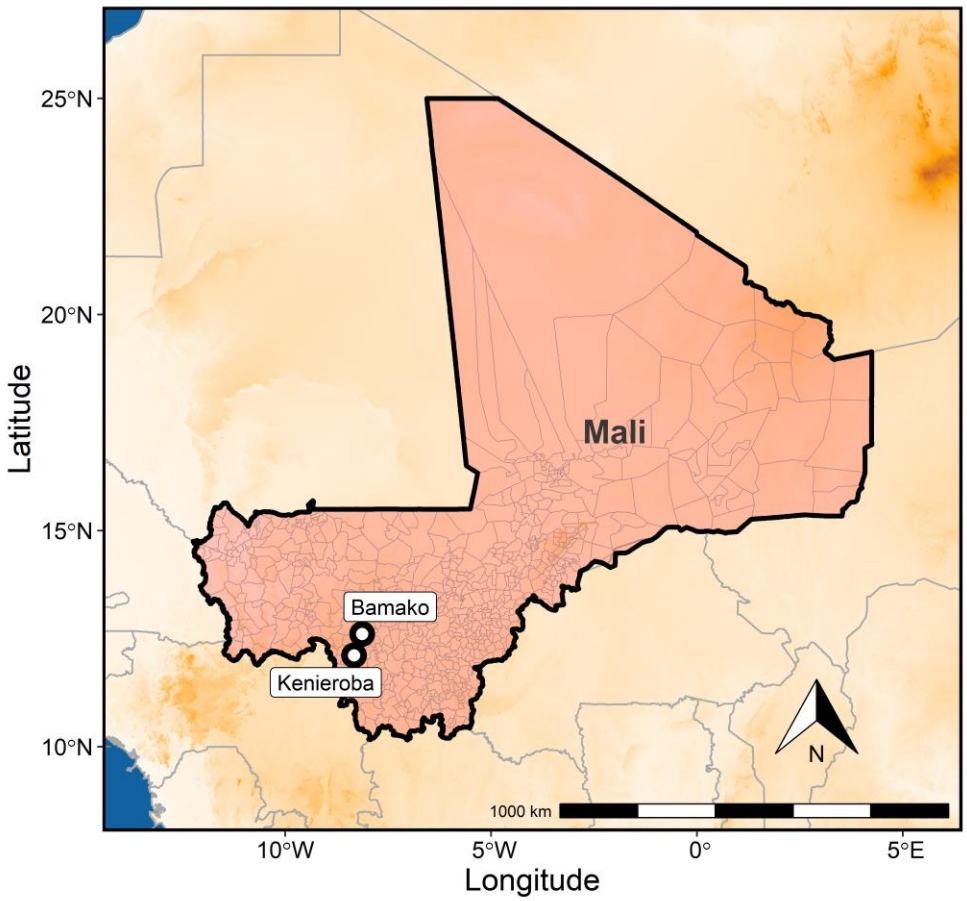

Figure 3: Map of Mali with study site Kenieroba and capital Bamako.

2.2 Participants

2.2.1 Malian Clinical Samples

Blood samples were collected from *Plasmodium falciparum* infected children aged two to 17 years living in Kenieroba, Mali. Inclusion criteria required participants be residents of Kenieroba, Mali, aged two to 17 years, infected with uncomplicated *P.*

falciparum confirmed by blood film, asexual parasite count between 2,000 and 200,000 parasites per microliter, and tympanic or axillary temperature greater than or equal to 37.5^{0}C or fever within 24 hours of the visit. Participants were excluded from the study if there were any signs of severe malaria, severe malnutrition, presence of *P. ovale* or *P. malariae* on blood film, acute illness requiring treatment, pregnant or breastfeeding, planning to become pregnant within one month, history of treatment with ACT in previous 14 days, known hypersensitivity to artemether or lumefantrine, splenectomy, co-administration of strong inducers of CYP3A4, any condition that in the opinion of the investigator would render the patient unable to comply with the protocol, and any health condition that in the opinion of the investigator would confound data analysis or pose unnecessary exposure risk to the subject.

2.2.2 Time Series Samples

Blood samples from four donors, two with HbAS genotype and two with HbAA genotype, were collected at Duke University Hospital for an *in vitro* time series experiment (IRB #Pro00007816) conducted by the Taylor lab.

2.3 Procedures

2.3.1 Clinical Sample Collection

Clinical samples were collected as a part of an observational study examining the efficacy of Artemether-Lumefantrine in the treatment of uncomplicated malaria in children aged two to 17 years in Kenieroba, Mali (ClinicalTrials.gov Identifier:

NCT02645604). Participants were notified of the study intentions and all associated risks during the consent process. Written informed consent was acquired from each participant's parent or guardian in addition to assent from participants aged 14-17 years. Prior to treatment, whole venous blood was collected from participants presenting with uncomplicated malaria. Blood samples were passed through cellulose columns[27] and the flow-through was stored in RNAprotect (Qiagen) in cryovials. This field study was approved by the Institutional Review Board of the University of Sciences, Techniques, and Technologies of Bamako (IRB #00001983).

2.3.2 Time Series Culturing

Time series samples were used to observe *Pf*CyP-19B expression over the course of 48 hours, corresponding with one complete parasite erythrocytic cycle. *Plasmodium falciparum* parasite strains were obtained from BEI Resources, NIAID, NIH. Daniel J. Carucci contributed strain 3D7 (MRA-102). *P. falciparum* parasites were cultured in human red blood cells in a low oxygen environment at 37^{0}C. Parasites were then synchronized to obtain 12mL of infected red blood cells (iRBC) at 2% parasitemia. To ensure parasites were between zero and three hours post invasion (hpi), schizonts were isolated via Percoll by adapting procedures from the Ring-stage Survival Assay.[28] Synchronized parasites were evenly distributed among four flasks containing 1.8mL of RBCs from the four blood donors (two HbAS, two HbAA). The cultures were left to incubate for three hours to allow infection of the new RBCs before being treated with

sorbitol to kill the remaining schizonts. The result from each flask was a 1.8mL pellet of iRBCs that was then resuspended in 15mL of ACM. 500μL of the resuspension was then aliquoted to three 12-well plates with each well containing 3.5mL of pre-warmed ACM and 50μL of iRBCs. Samples were harvested every three hours, up to 48 hours, with the first timepoint being taken after distribution onto the 12-well plates. At each timepoint, the harvested samples were resuspended in 1mL of TRIzol (Thermo Fisher) for further processing and analysis.

2.3.3 RNA Extraction

RNA extraction was performed on whole blood samples resuspended in 1mL of TRIzol (Thermo Fisher). After thorough homogenization of the cells with a 25 gauge blunt needle and 1mL syringe, the contents were spun down and the supernatant was drawn off for RNA extraction. Working on ice, 200μL of chloroform was added per 1mL TRIzol, microcentrifuge tubes were shaken vigorously by hand for 20 seconds, and then set to incubate at room temperature for three minutes before returning to ice. The tubes were then spun in a refrigerated microcentrifuge (Eppendorf) for 15 minutes at 12,000xg and 4^{0}C. On ice, the upper aqueous phase (approximately 600μL) was drawn off and placed in a new microcentrifuge tube where one volume of RNase-free 70% ethanol was added and the tube vortexed. RNeasy mini columns (Qiagen) were loaded, in two batches, and spun for 15 seconds at 8,000xg and at room temperature, flow-through was discarded. 350μL of buffer RW1 (Qiagen) was added to each column, columns were then

spun for 15 seconds at 8,000xg and at room temperature, flow-through was discarded. 80µL DNase (Qiagen) was added directly to the column membrane and samples were set to incubate at room temperature for 25 minutes. The samples were washed with 350µL of buffer RW1 (Qiagen), followed by 500µL of buffer RPE (Qiagen). RNA was eluted into 30µL of RNase-free water and RNA and DNA concentrations were measured using the Qubit RNA HS assay and the Qubit DS DNA HS assays, respectively. RNA was then stored at -80^{0}C for further processing.

2.3.4 Reverse Transcription

Reverse transcription was carried out using the AffinityScript QPCR cDNA Synthesis Kit (Agilent) and 6µL of extracted RNA sample. Reagents were added to a PCR tube in the following order: 10µL First Strand Mastermix, 3µL random primers, 1µL AffinityScript RT/RNase Block enzyme mixture, and 6µL RNA sample. Reverse transcription was executed on the Bio-Rad T100 ThermalCycler with the following conditions: 42^{0}C for five minutes, 55^{0}C for 15 minutes, 95^{0}C for five minutes, and held at 4^{0}C until being stored at -20^{0}C for further processing.

2.3.5 Assay Validation

The *Pf*CyP-19B quantification assay was drafted for use with the QuantStudio 6 real-time PCR machine (Thermo Fisher) and 384-well plates. Through a series of experiments, we validated the assay for use with the LightCycler®96 real-time PCR machine (Roche) and 96-well plates. Our qPCR assay was initially validated on the

LightCycler®96 by comparing qPCR results to identical samples that were run using the QuantStudio 6. A series of experiments was performed to both confirm successful creation of cDNA during reverse transcription as well as successful and similar amplification of the cDNA templates created from the same RNA extracts. Reverse transcription success was confirmed by measuring cDNA concentration on a SpectraMax® QuickDrop™ Spectrophotometer (MolecularDevices) and by amplification during qPCR.

RNA and DNA concentrations were measured on a Qubit (Thermo Fisher) after RNA extractions to ensure successful extraction and DNase treatment. Samples were found to contain trace amounts of DNA, so an extra validation step was taken to determine if a single DNase treatment was sufficient for downstream experiments. To do this, we performed qPCR on two of our extracted RNA samples before reverse transcription to check for DNA amplification with the reference p90 primer pair targeting *seryl-tRNA synthetase* gene transcripts.

Two experiments were conducted to further optimize the *Pf*CyP-19B assay for use with the LightCycler®96. The objective of the first optimization experiment was to decrease the cycle threshold (Ct) and cycle threshold error by increasing the volume of the template cDNA from 0.3µL/reaction to 0.6µL/reaction and 0.9µL/reaction. Total reaction volume was held constant at 12µL with increased cDNA volume being offset by an equal decrease in H_2O volume. All other experimental conditions were held constant,

samples were run in triplicate on a single 96-well plate to eliminate possible batch effects.

The next set of experiments were again designed to lower the Ct value and Ct error by doubling the total reaction volume from 12µL to 24µL with all other reaction conditions held constant. A volume adjustment in the qPCR program of the LightCycler®96 was made to reflect the increased reaction volume and therefore two batches were required. qPCR plates were prepared in a PCR cabinet at the same time, under the same conditions, and run on the same LightCycler®96 machine. Plate 1 with the original reaction volume (12µL) was run first while plate 2 with the doubled reaction volume (24µL) was stored in the 4^0C refrigerator and run immediately after plate 1.

2.3.6 qPCR

Our quantitative PCR (qPCR) protocol was optimized for use with a LightCycler®96 (Roche). Each reaction consisted of 6µL iTaq™ Universal SYBR Green Supermix (Bio-Rad), 0.3µL cDNA template, 4.5µL RNase-free water, and 1.2µL of either p90 or *Pf*CyP-19B primer (Table 1). qPCR was performed to quantify *Pf*CyP-19B gene expression relative to the reference gene *seryl-tRNA synthetase* (targeted by p90 primers). Each sample was run in triplicate with both p90 primers and *Pf*CyP-19B primers for a total of six reactions per sample. To ensure uniformity, a master mix was created for each sample and consisted of 42µL SYBR Green Supermix, 2.1µL template cDNA, and 31.5µL RNase-free water for a total volume of 75.6µL. Of the 75.6µL, half (37.8µL) was

transferred to a new microcentrifuge tube. One tube received either 4.2μL p90 or *Pf*CyP-19B primers, all tubes were labeled accordingly (Figure 4). 12μL of prepared reaction mixture was pipetted into a 96-well plate (Roche), in triplicate, for qPCR on the LightCycler®96 machine. No template controls (NTC) were created using a similar scheme but substituted RNase-free water for cDNA template (Figure 4). A no template control was included on each plate for both targets (p90 and *Pf*CyP-19B) and run in triplicate. To minimize batch effects, samples were randomly assigned to 96-well plates. qPCR was performed under the following conditions: Hold Stage: 50^0C for two minutes, 95^0C for 10 minutes; Amplification Stage (40 cycles): 95^0C for 15 seconds, 60^0C for one minute; Melt curve: 95^0C for 15 seconds, 60^0C for one minute, 0.05^0C/s, 95^0C for 15 seconds. Results were analyzed using the LightCycler®96 software (Roche, version 1.1) and a cycle threshold cutoff for a negative call was set at 35 cycles. This Ct cutoff of 35 cycles was determined post hoc. Eight of the 24 no template controls showed slight amplification after 35 cycles on the LightCycler®96. However, after analysis of melting peaks and control fluorescence relative to sample fluorescence, this amplification was deemed insignificant, justifying a negative call for all samples after 35 cycles.

Table 1: Primer information for p90 reference and *Pf*CyP-19B.

	p90 (reference)	PfCyP-19B
Gene Name	PF07_0073	PF3D7_1115600
Amplicon Size	153	133
GC% F/R	28/45	50/40
Tm F/R	54.84/56.66	58.34/55.3
Tm Melt	73.924	73.792
Forward	TCAATTTGATAAAGTGGAACAATTC	TGGCTCAAGGAGGAGACATT
Reverse	GCGTTGTTTAAAGCTCCTGA	TTTCCTGCATTAGCCATTGA

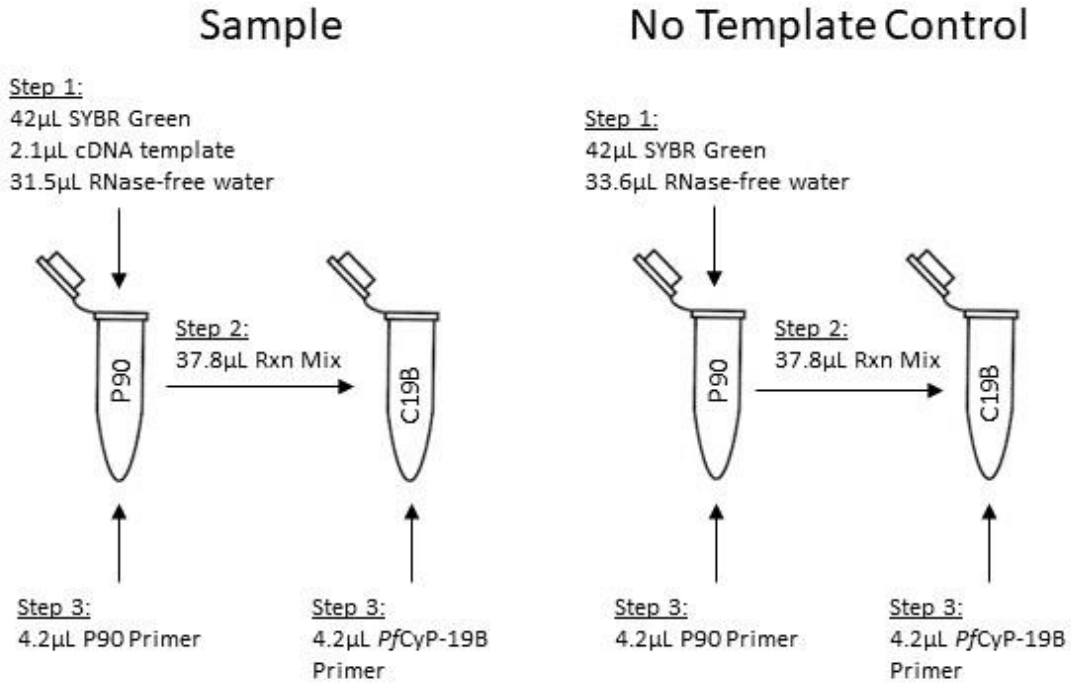

Figure 4: Schematic of the optimized master mix workflow used for qPCR.

2.4 Measures

2.4.1 Genotype

Hemoglobin genotype was determined in one of two ways for each study sample. *In vitro* time series samples were genotyped using Sanger sequencing, a three-step method involving chain termination PCR, size separation by gel electrophoresis, and fluorescence readout by a sequencing machine. Malian clinical samples underwent high performance liquid chromatography (HPLC) to determine hemoglobin genotype. HPLC is a standard blood test used to screen for hemoglobinopathies.

2.4.2 Transcript Units

Cyclophilin 19B transcript abundance was measured relative to the transcript level of the reference gene p90. qPCR was performed on each sample with six technical replicates, three replicates using the reference p90 primers and three replicates using the target *Pf*CyP-19B primers. Cycle threshold (Ct) values were obtained from the LightCycler®96. Delta cycle threshold (ΔCt) values were calculated for all *Pf*CyP-19B replicates using the equation: $\Delta Ct = Ct_{Pf\text{CyP-19B replicate}} - Ct_{p90\ mean}$. This equation takes the Ct of each individual *Pf*CyP-19B replicate minus the mean Ct value of the three corresponding p90 replicates. *Pf*CyP-19B transcript units for each sample replicate were then calculated using this ΔCt value in the equation $TU = 2^{(5-\Delta Ct)}$ where a value of 32 corresponds to the mean transcript level of the reference gene.[29] ΔCt and transcript units

were calculated for each sample replicate, translating to three measures of transcript units per sample. All ΔCt values and transcript units were calculated in Excel.

2.4.3 Parasite Stage

Parasite stage (ring, trophozoite, or schizont) was based on morphology assessed by light microscopy in the *in vitro* time series experiments. Peak transcripts were identified for each of the three stages of the *in vitro* parasites and used to estimate the developmental stage of the *in vivo* clinical samples from Mali.

2.5 Analysis

2.5.1 Sample Size

Sample size was limited due to available clinical and *in vitro* samples as analyses for this thesis were secondary to initial study objectives. However, due to the exploratory nature of this study the small sample sizes were justified and noted as a limitation.

2.5.2 Statistical Analysis

The primary outcome of interest for both *in vitro* time series samples and *in vivo* Malian clinical samples was transcript units calculated from qPCR cycle threshold values as described above. Among *in vivo* samples, transcript units were compared for significant differences in expression level between hemoglobin genotypes HbAA and HbAS using Wilcoxon rank sum (significance level α=0.05). Due to the small sample size of the *in vivo* data, bootstrapping methods were used to calculate a difference in medians

to confirm the magnitude and direction of the differences determined by Wilcoxon rank sum tests. These same methods were used to compare transcript units among trophozoite and ring stage parasites grown in HbAA and HbAS RBCs.

Time series data included the dependent continuous variable transcript units and independent categorical variable of time measured in eight six-hour blocks for both HbAA and HbAS genotypes. A response profile model was used to visualize the *Pf*CyP-19B expression over time in the two genotypes. Absolute and relative differences in mean transcript units were calculated between HbAA and HbAS genotypes. Absolute differences were calculated as mean TU HbAS minus mean TU HbAA per timepoint. Relative differences were calculated as follows: $\frac{(\mu TU\ HbAS - \mu TU\ HbAA)}{\mu TU\ HbAA} \times 100.$

2.5.3 Software

qPCR Ct values, Ct means, and Ct errors were obtained from the LightCycler®96 software (version 1.1) and exported as a CSV file for further analysis in Excel and R. Graphical figures and maps, unless otherwise indicated, were generated in RStudio (version 4.0.3) using the ggplot2 package. Wilcoxon rank sum analyses were performed using default packages that are loaded with RStudio. Bootstrapping analyses were carried out in RStudio using the boot package.

3. Results

3.1 Assay Validation

We first performed qPCR on extracted RNA samples to check for DNA amplification to determine if a single DNase treatment was sufficient. There was no amplification in either sample and fluorescence was consistent with the no template controls. A single DNase treatment during the RNA extraction protocol was deemed sufficient for removal of DNA.

Next, we compared Ct values of the same cDNA template amplified on both the LightCycler®96 and the QuantStudio 6 (Figure 5). Ct values were slightly higher on the LightCycler®96 but were of the same magnitude as Ct values from the QuantStudio 6. The increase in Ct value is likely due to multiple freeze-thaw cycles of the cDNA template that occurred after measurement on the QuantStudio 6 and before qPCR on the LightCycler®96.

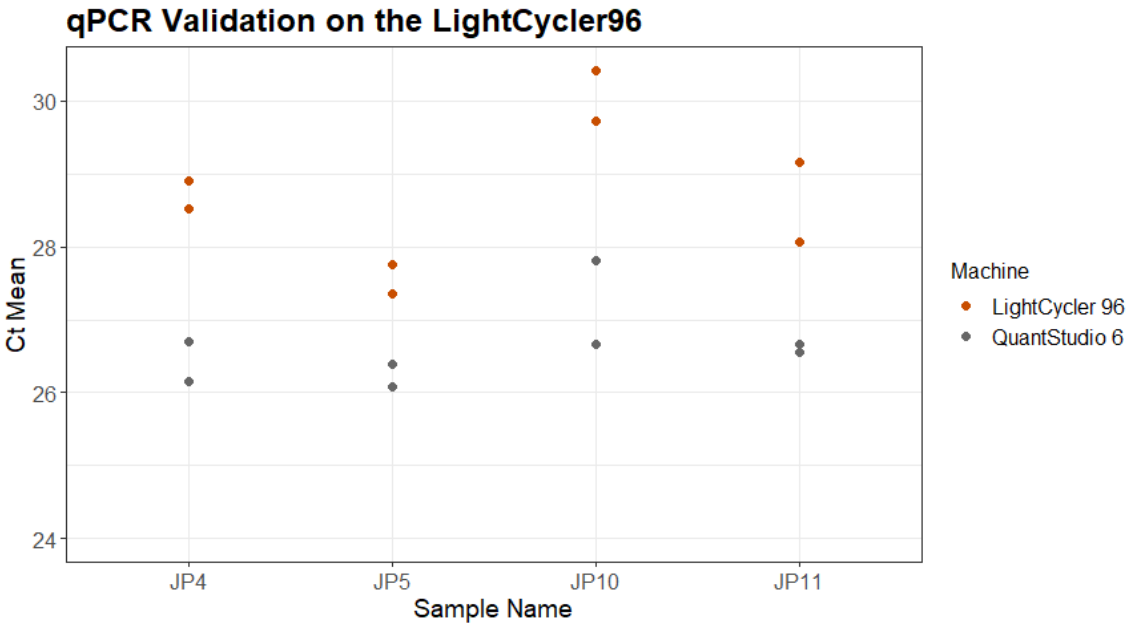

Figure 5: qPCR assay validation on the LightCycler®96. Four samples underwent qPCR on two real-time PCR machines. First, the QuantStudio 6 and later the LightCycler®96. Cycle threshold (Ct) mean values were compared between the two machines.

Two optimization experiments were performed to try to decrease the Ct value and Ct error during qPCR. Increasing the volume of template cDNA from 0.3µL/reaction to 0.6µL/reaction and 0.9µL/reaction had no effects on Ct value or Ct error that justified a change in protocol from the original 0.3µL cDNA template per reaction (Figure 6). There was no meaningful decrease in Ct value with increased cDNA concentration (Figure 6A). Additionally, Ct error increased with increased cDNA concentration (Figure 6B). When the total reaction volume was doubled from 12µL to 24µL, Ct values were not meaningfully different (Figure 7A) and Ct error increased slightly (Figure 7B). These

results did not warrant the use of extra reagents, so the original reaction volume of 12µL was used in all qPCR experiments.

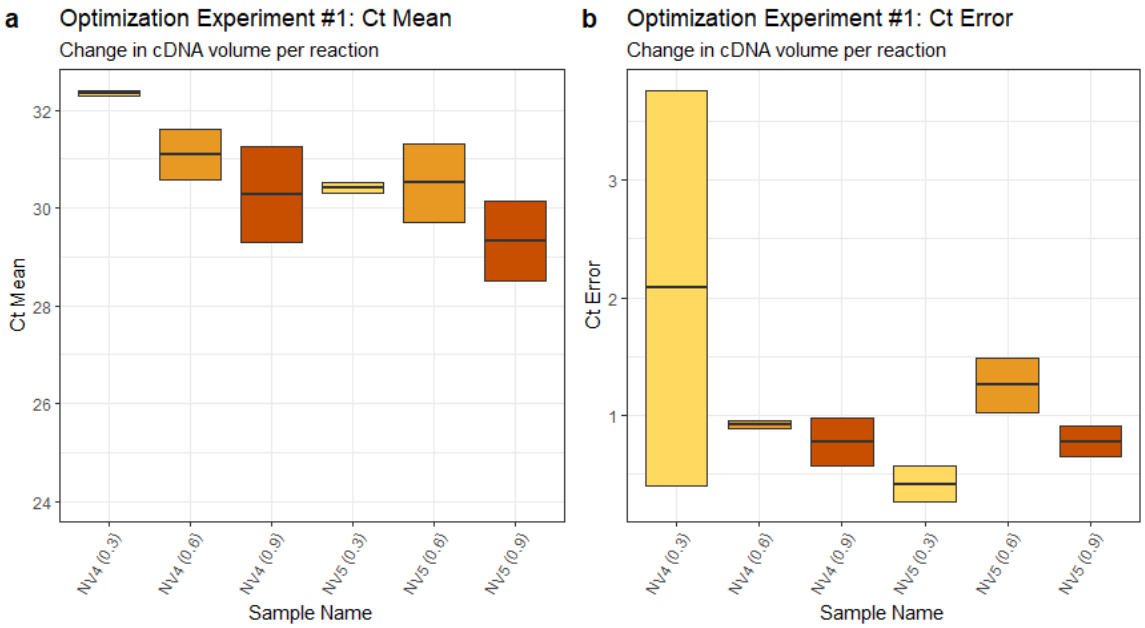

Figure 6: Results from the first qPCR optimization experiment, changing cDNA volume from 0.3µL/reaction to 0.6µL/reaction and 0.9µL/reaction. qPCR was performed on two different samples at each of the three cDNA volumes specified. Light orange represents the original volume of 0.3µL of cDNA, orange represents 0.6µL cDNA, and dark orange represents 0.9µL cDNA. Panel A: Cycle threshold (Ct) mean values per sample. Panel B: Ct error values per sample.

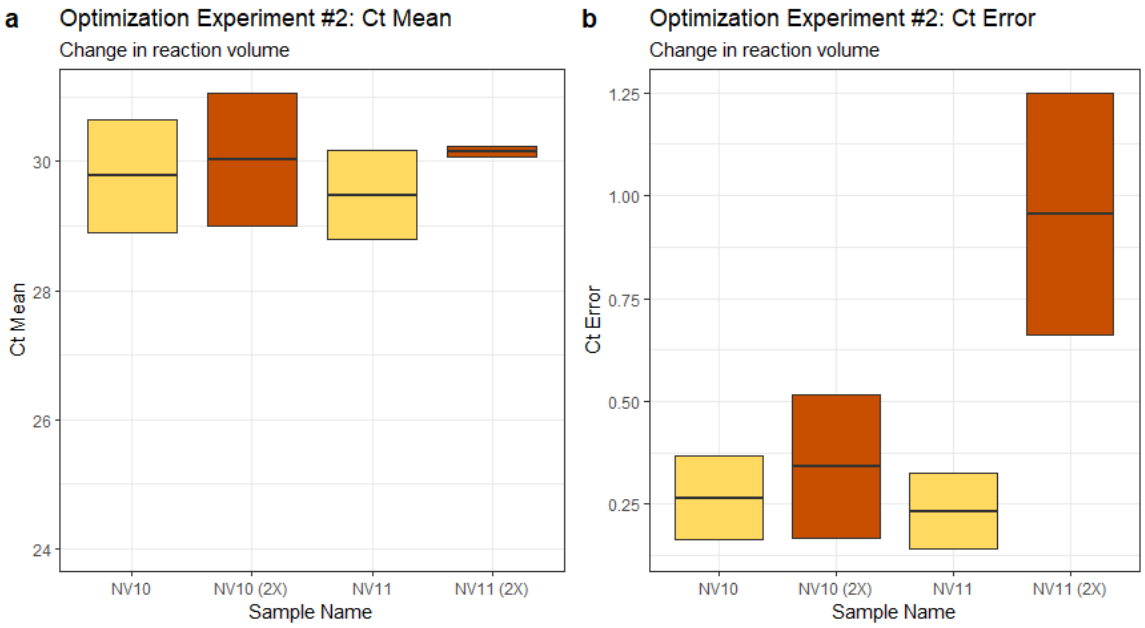

Figure 7: Results from the second qPCR optimization experiment, doubling the total reaction volume from 12µL to 24µL. Panel A: Ct mean values per sample. Panel B: Ct error values per sample.

3.2 Time Series Results

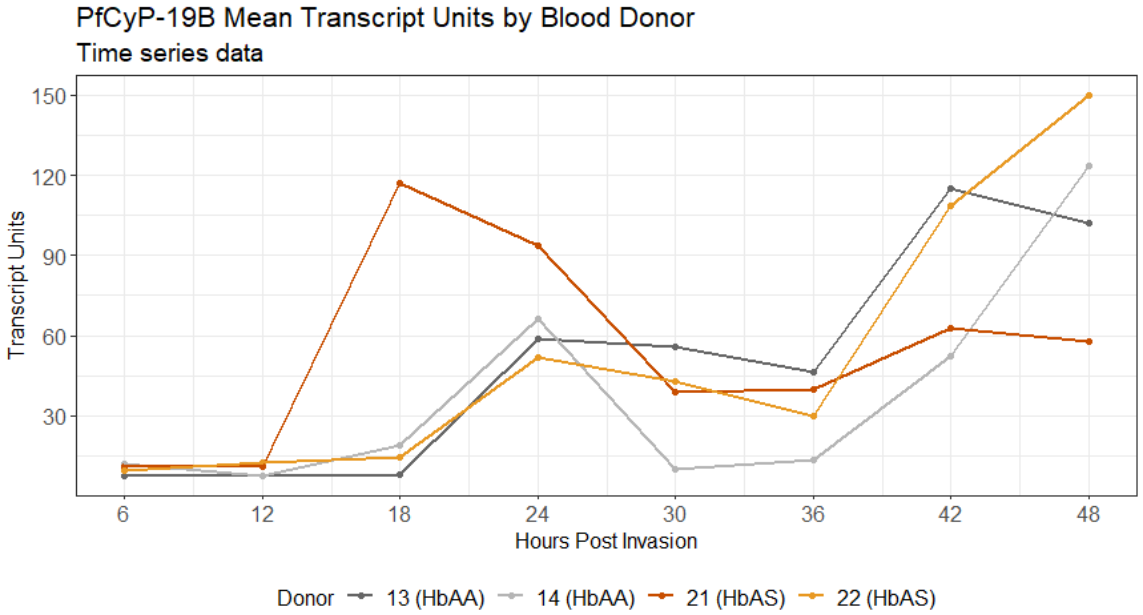

Figure 8: Individual donor mean cyclophilin 19B transcript units plotted by time point with the first time point being measured at six hours post invasion. Orange lines correspond to HbAS genotype donors and grey lines correspond to HbAA genotype donors.

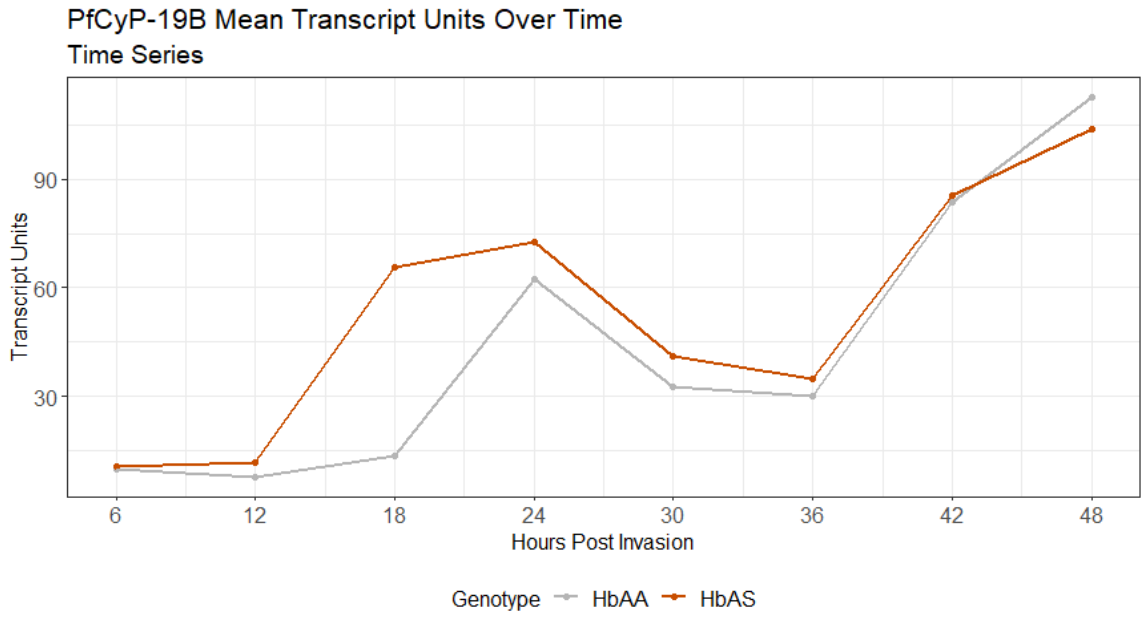

Figure 9: Mean cyclophilin 19B transcript units per genotype plotted by time point starting at six hours post invasion. The orange line corresponds to HbAS genotypes and the grey line corresponds to HbAA genotypes.

Table 2: *In vitro* HbAA and HbAS mean transcript units per timepoint. *Absolute difference calculated as mean transcript units of HbAS minus mean transcript units of HbAA. **Relative difference calculated as absolute difference divided by mean TU HbAA times 100.

Hours post invasion	HbAA mean transcript units, n=2 (St. dev.)	HbAS mean transcript units, n=2 (St. dev.)	Absolute difference in means*	Relative difference in means**
6	9.674 (3.369)	10.343 (3.241)	0.669	6.91%
12	7.426 (1.846)	11.585 (3.203)	4.159	56.01%
18	13.540 (8.146)	65.782 (58.565)	52.242	385.83%
24	62.379 (13.439)	72.549 (30.259)	10.170	16.30%
30	32.730 (30.390)	40.873 (10.357)	8.144	24.88%
36	30.082 (20.402)	34.791 (11.581)	4.709	15.65%
42	83.760 (51.999)	85.671 (35.339)	1.911	2.28%
48	112.897 (29.359)	103.966 (60.947)	-8.930	-7.91%

Time series samples were plotted over the 48-hour course of sample collection with six hours post invasion as the first timepoint (Figure 8). Although non-linear, transcript units tend to increase over time, regardless of genotype. There are two peaks in transcript units at 24 hours post invasion and at 48 hours post invasion when the samples are collapsed into mean data (Figure 9). Mean transcript units and standard deviations for each genotype are reported in Table 2 along with absolute and relative differences in means. At all timepoints up to, but not including 48 hours, mean transcript units are greater in the HbAS genotype compared to the HbAA genotype (Table 2). The two genotypes follow a similar pattern of expression excluding a stark contrast at 18 HPI where the relative difference in mean transcript units is nearly 400% with HbAS exhibiting greater expression than HbAA.

3.3 Mali Results

3.3.1 Transcript Units Across All Samples

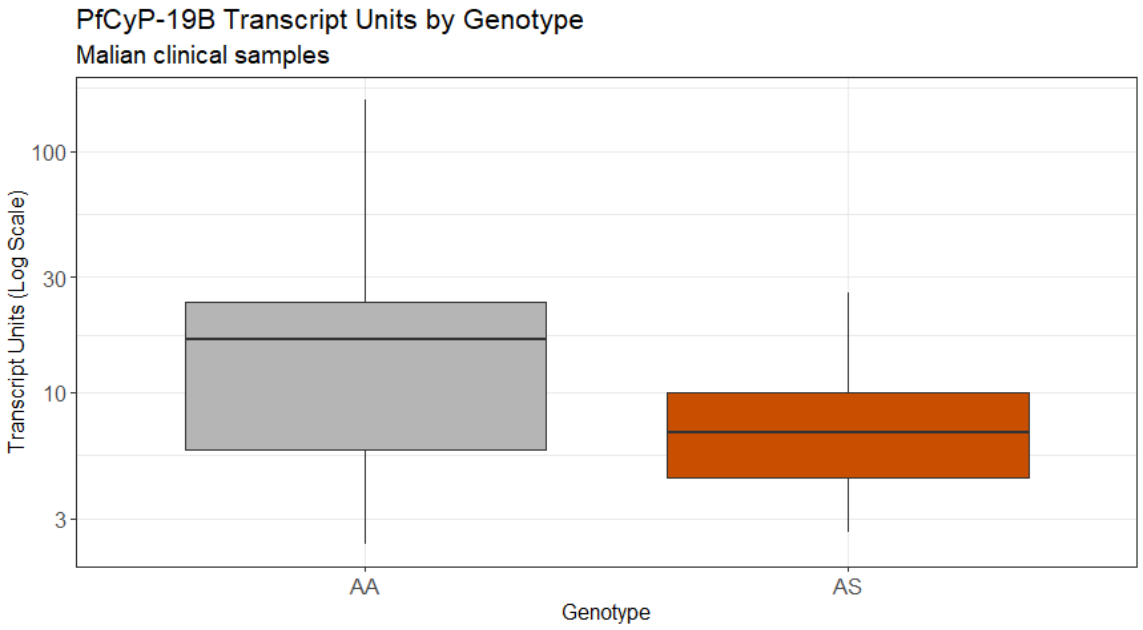

Figure 10: Cyclophilin 19B transcript units plotted by genotype. Grey represents the HbAA genotypes and orange represents the HbAS genotypes. Transcript units on the y-axis are represented on a log scale.

There was a total of 27 clinical samples that were processed for this study, 12 HbAA samples and 15 HbAS samples. The median transcript units for all HbAA and HbAS samples were 16.526 and 6.837, respectively. Mean transcript units for HbAA and HbAS samples were 26.598 and 8.660, respectively. There were outliers in both sample groups that were included in statistical analyses. Based on Wilcoxon rank sum (α=0.05), there was a statistically significant difference in median transcript units between genotypes, with lower median transcripts in HbAS compared to HbAA(p=0.006) (Figure 10). Bootstrapping methods were used to estimate the difference in median transcript

units between genotypes. Using the boot package in RStudio with 1000 replicates, a difference in median transcript units between HbAA and HbAS was estimated to be 8.95 (95% CI: 0.05, 13.34) indicating lower expression of *Pf*CyP-19B among the HbAS genotype compared to the HbAA genotype.

3.3.2 Transcript Units by Parasite Stage

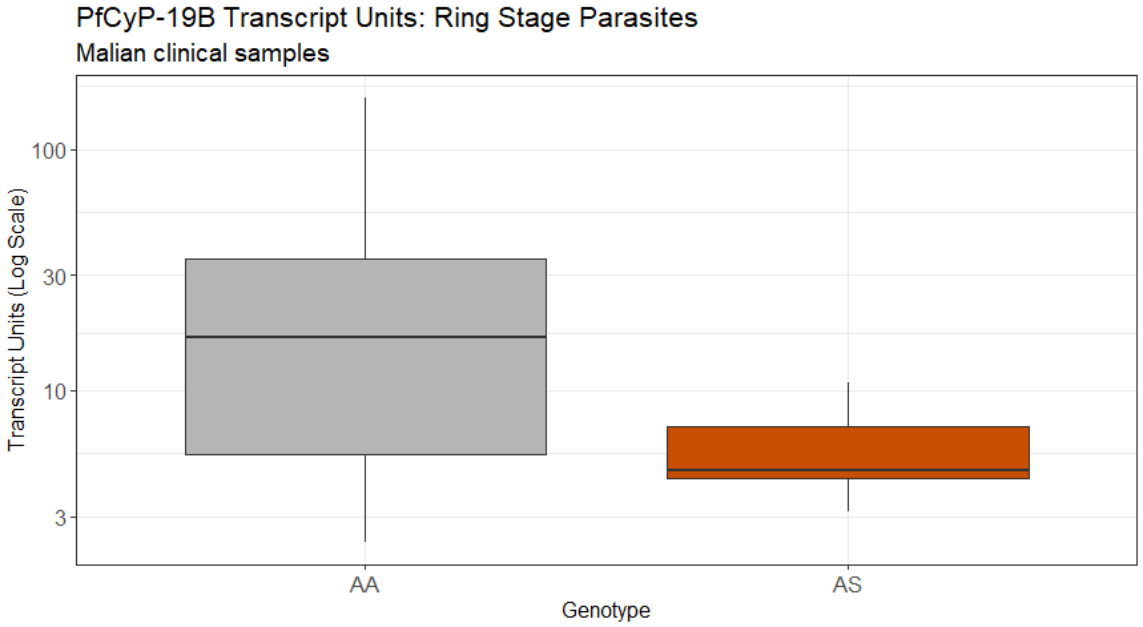

Figure 11: Cyclophilin 19B transcript units among ring stage parasites plotted by genotype. Grey represents the HbAA genotypes and orange represents the HbAS genotypes. Transcript units on the y-axis are represented on a log scale.

Parasites were classified as either ring stage or trophozoite stage as described in the methods. There were eight HbAS samples and eight HbAA samples that were classified as rings. Mean and median transcript units for ring stage parasites within the sample group of HbAA genotype were 33.562 and 16.699, respectively, with three outliers that were included in calculations. Mean and median transcript units for ring

stage parasites within the sample group of HbAS genotype were 5.711 and 4.643, respectively, with no outliers. A difference in medians between ring stage transcript units among HbAA and HbAS was found to be statistically significant using Wilcoxon rank sum (p=0.005) with smaller median transcript units among HbAS rings compared to HbAA rings (Figure 11). Bootstrapping methods estimated a difference in medians of 11.90 (95% CI: 0.87, 21.30) indicating lower *Pf*CyP-19B expression in the HbAS genotype compared to the HbAA genotype in ring stage parasites.

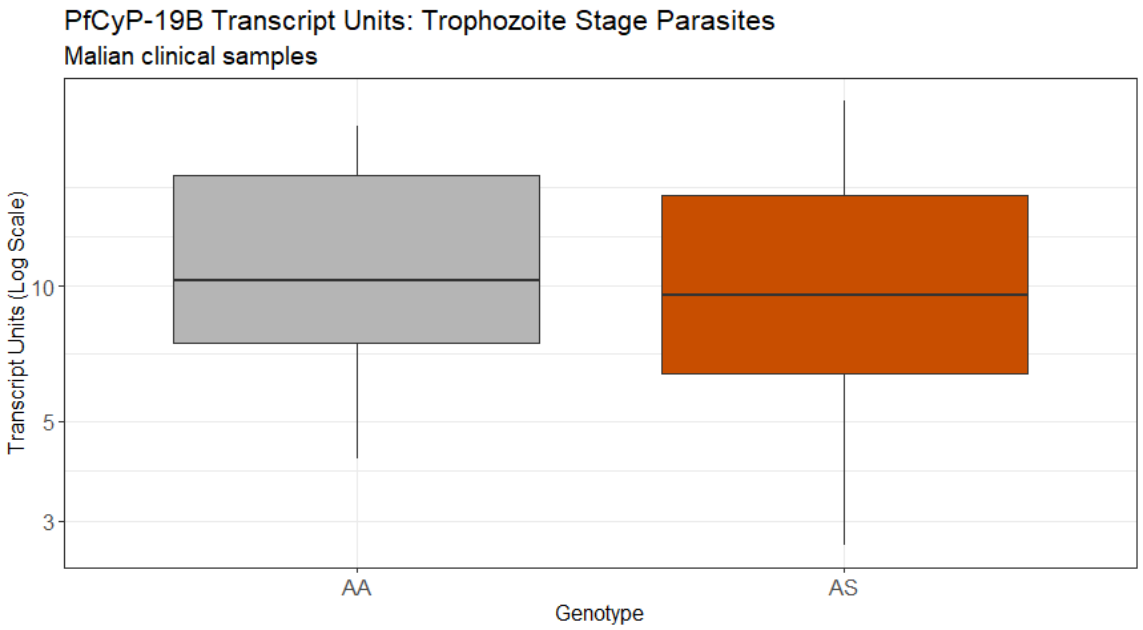

Figure 12: Cyclophilin 19B transcript units among trophozoite stage parasites plotted by genotype. Grey represents HbAA genotypes and orange represents HbAS genotypes. Transcript units on the y-axis are represented on a log scale.

There were seven HbAS samples and four HbAA samples classified as trophozoite stage parasites. Mean and median transcript units for trophozoite stage parasites in HbAA samples were 12.671 and 10.534, respectively, with no outlying data

points. Mean and median transcript units for trophozoite stage parasites in HbAS samples were 12.029 and 9.536, respectively, with no outliers. There was no significant difference in median transcript units among trophozoite stage parasites across genotypes (Wilcoxon rank sum p=0.926) (Figure 12). Bootstrapping methods returned a difference in medians of 0.71 (95% CI: -5.82, 9.14). The 95% confidence interval for the difference in medians includes zero, supporting the conclusion that *Pf*CyP-19B expression does not differ by genotype in trophozoite stage parasites.

3.3.3 Genotype Specific Transcript Units

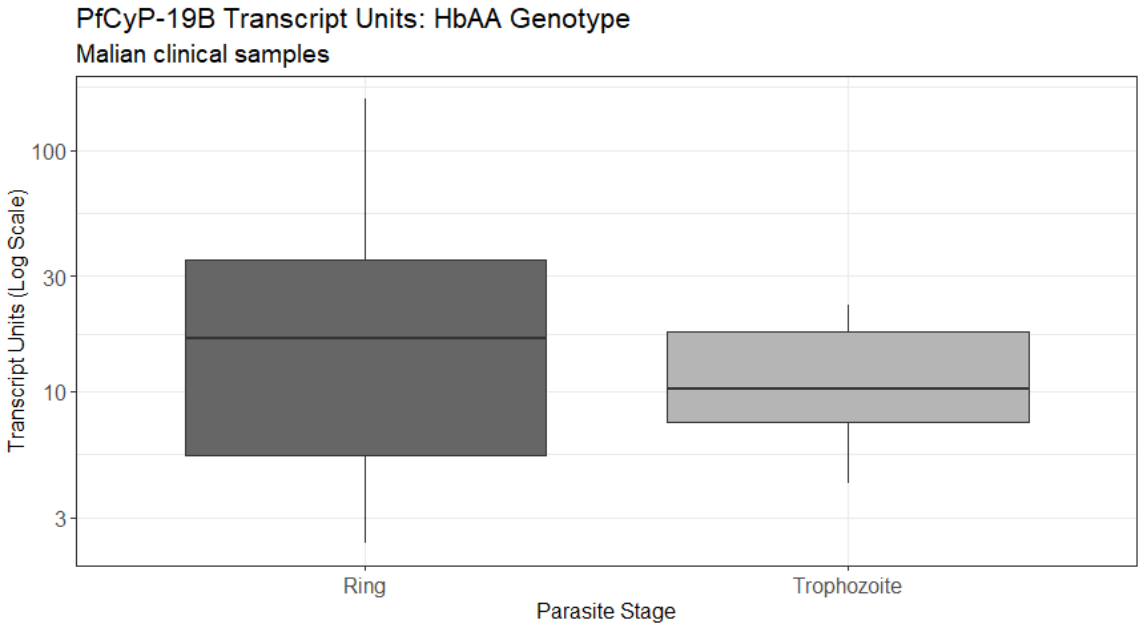

Figure 13: Cyclophilin 19B transcript units among parasites in participants with HbAA genotype plotted by parasite stage. Dark grey represents ring stage parasites and light grey represents trophozoite stage parasites. Transcript units on the y-axis are represented on a log scale.

Among the HbAA genotype, transcript units were analyzed by parasite stage, either ring (eight samples) or trophozoite (four samples). Mean and median transcript units for ring stage parasites were 33.562 and 16.699, respectively. Outlying data points were included in the summary statistic calculations. Mean and median transcript units for trophozoite stage parasites were 12.671 and 10.534, respectively, with no outliers. There was no significant difference in median transcript units between ring and trophozoite stage parasites among those with the HbAA genotype (Wilcoxon rank sum, p=0.603) (Figure 13). Bootstrapping methods estimated a difference in medians of 6.05 (95% CI: -8.91. 17.59). The inclusion of zero in the 95% confidence interval supports the conclusion that *Pf*CyP-19B expression does not vary by parasite stage in the HbAA genotype.

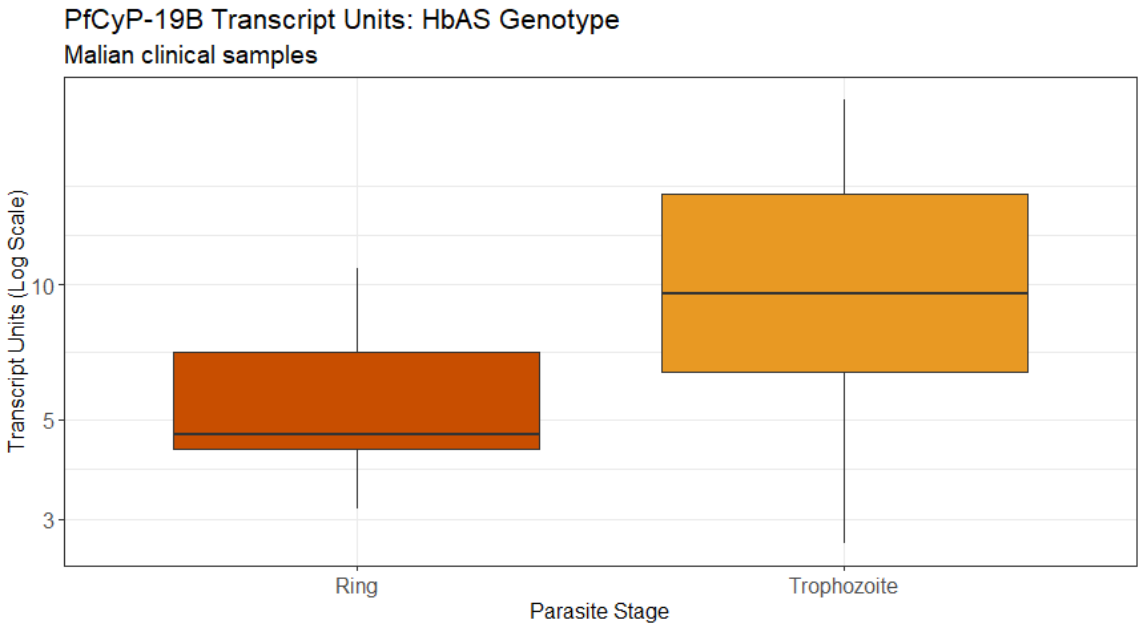

Figure 14: Cyclophilin 19B transcript units among parasites in participants with HbAS genotype plotted by parasite stage. Dark orange represents ring stage parasites and light orange represents trophozoite stage parasites. Transcript units on the y-axis are represented on a log scale.

Transcript units were calculated for ring stage (eight samples) and trophozoite stage (seven samples) parasites among those with the HbAS genotype. Mean and median transcript units for ring stage parasites were 5.711 and 4.643, respectively. Mean and median transcript units for trophozoite stage parasites were 12.029 and 9.536, respectively. There were no outliers in either parasite stage among HbAS genotype samples. There was a statistically significant difference in median transcript units between ring stage and trophozoite stage parasites with ring stage parasites having lower median transcript units than trophozoites among HbAS clinical samples (Wilcoxon rank sum, p=0.002) (Figure 14). Bootstrapping methods estimated a difference

in medians to be -4.80 (95% CI: -10.66, -2.05) indicating lower *Pf*CyP-19B expression among ring stage parasites when compared to trophozoite stage parasites for the HbAS genotype.

4. Discussion

4.1 Overview of Key Findings

Despite being a disease that has been studied for decades, malaria continues to kill hundreds of thousands of people annually, mostly children under the age of five. In geographic areas that have been heavily burdened by malaria, natural selection has favored specific genotypes that provide partial protection against severe malarial disease. One such genotype is the hemoglobin sickle-cell trait, HbAS. Multiple mechanisms have been proposed as to how HbAS confers protection, but the answer to this question is still unclear. Separately, cyclophilin 19B is a gene expressed by *P. falciparum* parasites and is thought to be an important component of the unfolded protein response of the parasite. While *Pf*CyP-19B has been studied in the context of artemisinin resistance, it has yet to be studied in depth alongside the sickle-cell trait.

The objective of our study was to determine if there is a relationship between *Pf*CyP-19B expression and the sickle-cell trait genotype. This study served two purposes: first, to explore the possible role *Pf*CyP-19B might have in the biological mechanisms that confer protection against severe malaria in individuals with HbAS genotype, and second, to contribute to the working knowledge of cyclophilin 19B in the *P. falciparum* parasite. Our main findings show decreased expression of *Pf*CyP-19B among HbAS genotype compared to HbAA genotype in clinical samples from Mali. Conversely, our time series experiment showed no significant difference in *Pf*CyP-19B expression

between genotypes. However, the time series results showed a 24-hour interval in peak expression of *Pf*CyP-19B in both genotypes.

4.2 PfCyP-19B Expression in Malian Clinical Samples

Using transcript units as a measure of gene expression, our overall results from the Malian clinical samples showed decreased *Pf*CyP-19B expression among parasites in HbAS samples compared to HbAA samples. These findings support our hypothesis that *Pf*CyP-19B expression would be significantly lower in individuals with the sickle-cell trait genotype.

As discussed previously, *Pf*CyP-19B is part of the parasitic unfolded protein response (UPR) and was found to be over expressed, along with other members of the UPR, in artemisinin-resistant parasites in Southeast Asia.[23] This up-regulation of the UPR seen in artemisinin-resistant parasites is thought to be the result of mutant kelch-13 proteins that exhibit an inhibited ability to negatively regulate the signal transductase pathway that triggers the UPR.[23] The lack of artemisinin-resistant parasites in Mali, coupled with the results of this experiment indicate that the change in *Pf*CyP-19B expression is due to the RBC environment rather than mutations in the parasitic genome. However, this would have to be confirmed with K13 sequencing of the parasites causing infection in each participant.

*Pf*CyP-19B is known to function as part of the *Plasmodium* reactive oxidative stress complex (PROSC), a protein chaperone complex that has been found to be up-

regulated in artemisinin-resistant parasites to respond to the oxidative pressures enforced by artemisinin.[23] Prior studies have shown that HbAS RBCs are prone to oxidation, causing an abundance of oxidants including free heme, hemichromes, and free iron.[30,31] In a harsh oxidative environment such as this, one would hypothesize PROSC to be up-regulated as is the case with artemisinin-resistant parasites. However, our results of decreased *Pf*CyP-19B expression indicate the opposite may be occurring. A decrease in PROSC activity would limit the parasites' ability to respond to the oxidative pressures of the HbAS RBC environment, thus resulting in increased parasite death and lower parasite density.[32,33] While this proposed mechanism may contribute in part to the protection conferred by HbAS genotype, due to the fact that similar parasite densities have been reported in both patients with HbAS and those with HbAA[9] it is not likely to be the predominant contributor to the protections afforded by HbAS genotype.

This leads us to speculate on the role that *Pf*CyP-19B and the UPR play in cytoadherence and protein export. An iRBC's ability to undergo cytoadherence to the endothelial vasculature is affected by the abundance of PfEMP-1 on the erythrocyte surface.[34,35] From prior studies, we know that HbAS iRBCs exhibit impaired export of proteins via Mauer's clefts, including the export of PfEMP-1 to the erythrocytic surface.[18] It is possible that certain cellular conditions of the HbAS erythrocyte are triggering a down-regulation of the parasitic UPR, as evidenced by decreased expression of *Pf*CyP-19B, that is in turn connected with the impaired export of proteins seen in HbAS

genotypes. Furthermore, if the UPR has limited function in HbAS RBCs, this could be directly limiting the export of PfEMP-1 and other proteins that mediate cytoadherence. If this is true, the UPR and perhaps specifically *Pf*CyP-19B, could prove to be effective therapeutic targets against severe *P. falciparum* malaria. Further research is required to investigate these potential associations and what aspects of the HbAS RBC could be triggering down-regulation of the UPR and thus decreased expression of *Pf*CyP-19B.

4.3 PfCyP-19B Expression in Time Series Samples

Our time series experiment produced mixed results with quite a bit of variance between sample replicates. When comparing mean transcript units across the four blood donors (two HbAA and two HbAS) we see that *Pf*CyP-19B expression is greater in HbAS samples compared to HbAA samples, up until the 48-hour time point. These findings are contrary to our hypothesis and the results from our *in vivo* clinical experiment. Although the variance between sample replicates is high, there are two distinct patterns that can be discerned from the data. First, while there are increases and decreases in *Pf*CyP-19B expression over time, there is an overall increase in transcript units from 6 hours post invasion to 48 hours post invasion seen in both genotypes. Second, there are two distinct peaks in expression at 24 hours post invasion and 48 hours post invasion for both genotypes.

P. falciparum has an asexual life cycle that takes approximately 48 hours to complete, from the time an erythrocyte is infected to the rupture of the schizont

releasing merozoites.[36] At approximately 24 hours post invasion, the ring stage parasites start to transition to trophozoites.[37] This ring to trophozoite transition state aligns with the first peak expression of *Pf*CyP-19B we saw in our time series experiment. Around 48 hours post invasion the mature schizont ruptures, causing the iRBC to burst and release merozoites back into the bloodstream to infect other RBCs and continue the life cycle. From 36 to 48 hours post invasion we saw a sharp increase in *Pf*CyP-19B expression aligning with this transition from trophozoite to ruptured schizont. Our results indicate that peak *Pf*CyP-19B expression aligns with transition states of the *P. falciparum* parasite, suggesting that *Pf*CyP-19B may play a role in aiding parasitic transitions. However, it is difficult to speculate the true significance of the 24-hour interval in peak expression due to our small sample size and the large variation we saw in our data.

P. falciparum parasites are often synchronized within the human host, as such, iRBCs burst at similar timepoints releasing merozoites into the blood stream, stimulating an immune response that results in the classic cyclical fever seen in malaria patients.[38,39] For *P. falciparum*, this fever typically occurs every 48 hours, in line with the asexual cell cycle. While our results show that maximum *Pf*CyP-19B expression occurs at 48 hours post invasion, given the understood function of cyclophilin 19B in the parasite, it is less likely to be a direct driver of disease manifestation and rather an indirect mediator through its role in the unfolded protein response. If there is a link between cyclophilin 19B and clinical disease, it is likely to be indirect, perhaps, as suggested by

our time series results, by aiding in parasitic transition states, or through its possible connection with protein export and cytoadherence as hypothesized by our Malian clinical results.

4.4 Divergent Findings Between In Vivo and In Vitro Results

The results from our *in vitro* Mali study supported our hypothesis of decreased cyclophilin 19B expression among sickle-trait genotypes. However, our time series results showed no substantial difference in expression between normal and sickle-trait genotypes. While these divergent findings are surprising, there are a few fundamental differences between the *in vivo* and *in vitro* environments that could account for the differential expression we observed *in vivo* but not *in vitro.* The *in vitro* environment is a protected culture of red blood cells into which a single parasite strain is inoculated. The parasites are nurtured under conditions that allow them to thrive. *In vitro* there is no competition with the human immune system nor any co-infections that may occur naturally. Conversely, our *in vivo* samples were collected from a malaria endemic region and it is quite possible that individuals were infected with multiple parasite strains. Additionally, the parasite densities were likely much higher among the *in vivo* samples as the duration of infection was longer compared to *in vitro* samples.

Aside from the environmental differences, the sample size was much smaller in the *in vitro* time series study with four total samples, two of each genotype. From a statistical standpoint, the true measure of effect is harder to estimate with smaller

sample sizes. Thus, larger sample sizes are preferred as the results are more generalizable to the population as a whole. It is possible that with a larger sample size, we would have observed similar differential cyclophilin 19B expression *in vitro* as we did *in vivo*.

4.5 Secondary Results from Malian Clinical Samples

4.5.1 Expression by Parasite Stage

When the Mali results were separated into ring stage parasites and trophozoite stage parasites, we saw a significant difference in *Pf*CyP-19B expression between HbAS and HbAA genotypes in ring stage parasites but not in trophozoite stage parasites. Among the ring stage parasites, *Pf*CyP-19B expression was lower in HbAS samples compared to HbAA samples, with more variability in transcript units in the HbAA ring stage parasites. These results indicate that the overall differences in *Pf*CyP-19B expression between HbAA and HbAS genotypes are due to differential expression in the ring stage rather than the trophozoite stage. During the ring stage of the parasite life cycle, expression peaks for parasitic proteins that are exported into the host as host cell modifications take place.[40] It is interesting then, that *Pf*CyP-19B expression is decreased in this stage within HbAS RBCs and suggests, if cyclophilin 19B is associated with protein export, that parasitic modifications of the host cell may be limited.

4.5.2 Expression by Genotype

We further analyzed the Mali samples by parasite stage within each genotype and found a significant difference in *Pf*CyP-19B expression levels between ring stage and trophozoite stage parasites within the HbAS genotype, but no such difference in expression level within the HbAA genotype. Our HbAS results showed lower expression in the ring stage parasites than in the trophozoites. This suggests that *Pf*CyP-19B expression is relatively constant in parasites growing in HbAA RBCs while expression increases from ring stage to trophozoite stage in parasites growing in HbAS RBCs. This pattern seen in the HbAS genotype supports expression patterns seen in our time series experiment with increased expression in the later stages of parasite development. However, as these are cross-sectional data, strong inferences cannot be made about time dependent outcomes.

4.6 Assay Validation

The beginning phase of this study required the validation and optimization of our *Pf*CyP-19B quantification assay. Through a series of experiments, we were able to finalize the two-step reverse transcription and qPCR assay for accurate quantification of *Pf*CyP-19B using RNA extracted from whole blood. Our intended use of this assay was to study the expression of *Pf*CyP-19B among parasites grown in normal and sickle-trait blood. However, this is a versatile assay that can be used to study *Pf*CyP-19B in a variety of contexts. As mentioned previously, cyclophilin 19B is thought to play a role in *P.*

falciparum parasites that are resistant to artemisinin.[23] Our quantification assay can be used to study *Pf*CyP-19B expression in parasites that are resistant or susceptible to artemisinin, potentially adding valuable insights into the parasitic mechanisms of resistance to this first-line treatment.

4.7 Study Limitations

Our study faced a few limitations that may restrict the generalizability of our findings. In both sample sets, *in vitro* time series samples and *in vivo* Malian clinical samples, our sample size was small and was restricted by time and available resources. However, as the purpose of this research was exploratory and meant as a starting point for further investigation into the role of *Pf*Cyp-19B, smaller sample sizes are justified. It is also possible that our results were constrained by batch effects as not all samples could undergo qPCR on the same 96-well plate. To mitigate any possible batch effects, time series samples were randomized among four different plates to ensure a mix of timepoints and sample blood donors on each plate. Likewise, Malian clinical samples were randomized to two plates with a mix of HbAA and HbAS genotypes on each plate. Though this randomization does not eliminate batch effects, it balances batch effects by distributing them across samples and timepoints.

4.8 Future Experiments

To further investigate the role of *Pf*CyP-19B in the HbAS genotype, one could perform a knock-out experiment in which the cyclophilin 19B gene is knocked out and *in*

vitro RBCs from HbAA and HbAS donors are inoculated with either the knock-out or wild type parasites. Several factors could be measured and analyzed between the KO and WT parasites, of particular interest would be measuring the levels of the protein PfEMP-1 as it plays a vital role in cytoadherence. Additionally, it would be interesting to study *Pf*CyP-19B expression levels in other hemoglobinopathies that confer partial protection against *P. falciparum* malaria. Moreover, extending the length of our time series experiment would allow us to investigate if the 24-hour interval of peak expression continues. As previously noted, *Pf*CyP-19B expression is up-regulated in artemisinin-resistant parasites.[23] It would be interesting to study the effects of *Pf*CyP-19B expression when HbAS RBCs are inoculated with artemisinin-resistant *P. falciparum* parasites.

A secondary component of this thesis was intended to be the implementation of our quantification assay with artemisinin-resistant parasites from Myanmar collected on dried blood spots (DBS). Due to time constraints and adverse storage conditions of DBS samples available to us, this did not come to fruition. The limiting step was RNA extraction from the DBS samples. Further experimentation with RNA extraction from DBS protocols and downstream validation of our quantification assay with said RNA extracts would prove valuable as DBS samples are much easier to collect, store, and transport than whole blood. Similarly, artemisinin resistance poses a serious threat to malaria elimination efforts in the Greater Mekong Subregion of Southeast Asia.[2] Further

research can be conducted using our *Pf*CyP-19B quantification assay to study the role of *Pf*CyP-19B in artemisinin-resistant parasites.

5. Conclusion

Consistent with our hypothesis, in our clinical samples from Malian children we observed decreased *Pf*CyP-19B transcript expression among parasites in children with the HbAS genotype compared to children with the HbAA genotype. These results suggest that cyclophilin 19B and its role in the unfolded protein response could be contributing to the biological mechanisms that confer protection against severe malaria in those with the HbAS genotype. Future studies should investigate this association further, with an emphasis on the link between *Pf*CyP-19B and the export of PfEMP-1 to the erythrocyte surface. Though our time series experiment did not show any significant differences in *Pf*CyP-19B expression between HbAA and HbAS genotypes as we expected, the results did reveal an overall increase in expression over time with peak expression at 24-hour intervals. To investigate the significance of these expression peaks further, extended time series experiments should be carried out. With this study we were able to explore *Pf*CyP-19B expression levels in parasites growing in HbAA and HbAS RBCs and conclude that parasites in HbAS RBCs exhibit decreased *Pf*CyP-19B expression *in vivo*. It will be important to continue building on this foundational knowledge to better understand the diverse role of cyclophilin 19B within the parasite and in relation to artemisinin resistance.

References

1. Cox, F. E. History of the discovery of the malaria parasites and their vectors. *Parasit. Vectors* **3**, 5 (2010).

2. World malaria report 2020: 20 years of global progress and challenges. (2020).

3. Bousema, T. & Drakeley, C. Epidemiology and Infectivity of Plasmodium falciparum and Plasmodium vivax Gametocytes in Relation to Malaria Control and Elimination. *Clin. Microbiol. Rev.* **24**, 377–410 (2011).

4. Information, N. C. for B., Pike, U. S. N. L. of M. 8600 R., MD, B. & Usa, 20894. *CLINICAL MALARIA AND EPIDEMIOLOGY*. *Guidelines for the Treatment of Malaria. 3rd edition* (World Health Organization, 2015).

5. Carlson, J. *et al.* Human cerebral malaria: association with erythrocyte rosetting and lack of anti-rosetting antibodies. *Lancet Lond. Engl.* **336**, 1457–1460 (1990).

6. Institute of Medicine (US) Committee on the Economics of Antimalarial Drugs. *Saving Lives, Buying Time: Economics of Malaria Drugs in an Age of Resistance*. (National Academies Press (US), 2004).

7. Murayama, M. Structure of Sickle Cell Hemoglobin and Molecular Mechanism of the Sickling Phenomenon. *Clin. Chem.* **13**, 578–588 (1967).

8. Modell, B. & Darlison, M. Global epidemiology of haemoglobin disorders and derived service indicators. *Bull. World Health Organ.* **86**, 480–487 (2008).

9. Taylor, S. M., Parobek, C. M. & Fairhurst, R. M. Haemoglobinopathies and the clinical epidemiology of malaria: a systematic review and meta-analysis. *Lancet Infect. Dis.* **12**, 457–468 (2012).

10. Beet, E. A. Sickle cell disease in the Balovale District of Northern Rhodesia. *East Afr. Med. J.* **23**, 75–86 (1946).

11. Luzzatto, L., Nwachuku-Jarrett, E. S. & Reddy, S. INCREASED SICKLING OF PARASITISED ERYTHROCYTES AS MECHANISM OF RESISTANCE AGAINST MALARIA IN THE SICKLE-CELL TRAIT. *The Lancet* **295**, 319–322 (1970).

12. Roth, E. F. *et al.* Sickling rates of human AS red cells infected in vitro with Plasmodium falciparum malaria. *Science* **202**, 650–652 (1978).

13. Gong, L., Parikh, S., Rosenthal, P. J. & Greenhouse, B. Biochemical and immunological mechanisms by which sickle cell trait protects against malaria. *Malar. J.* **12**, 317 (2013).

14. Orjih, A. U., Chevli, R. & Fitch, C. D. Toxic heme in sickle cells: an explanation for death of malaria parasites. *Am. J. Trop. Med. Hyg.* **34**, 223–227 (1985).

15. Ginsburg, H., Handeli, S., Friedman, S., Gorodetsky, R. & Krugliak, M. Effects of red blood cell potassium and hypertonicity on the growth of Plasmodium falciparum in culture. *Z. Parasitenkd. Berl. Ger.* **72**, 185–199 (1986).

16. LaMonte, G. *et al.* Translocation of sickle cell erythrocyte microRNAs into Plasmodium falciparum inhibits parasite translation and contributes to malaria resistance. *Cell Host Microbe* **12**, 187–199 (2012).

17. Cholera, R. *et al.* Impaired cytoadherence of Plasmodium falciparum-infected erythrocytes containing sickle hemoglobin. *Proc. Natl. Acad. Sci. U. S. A.* **105**, 991–996 (2008).

18. Kilian, N. *et al.* Hemoglobin S and C affect protein export in Plasmodium falciparum-infected erythrocytes. *Biol. Open* **4**, 400–410 (2015).

19. Wang, P. & Heitman, J. The cyclophilins. *Genome Biol.* **6**, 226 (2005).

20. Marín-Menéndez, A. & Bell, A. Overexpression, purification and assessment of cyclosporin binding of a family of cyclophilins and cyclophilin-like proteins of the human malarial parasite Plasmodium falciparum. *Protein Expr. Purif.* **78**, 225–234 (2011).

21. Gavigan, C. S., Kiely, S. P., Hirtzlin, J. & Bell, A. Cyclosporin-binding proteins of Plasmodium falciparum. *Int. J. Parasitol.* **33**, 987–996 (2003).

22. Hirtzlin, J., Färber, P. M., Franklin, R. M. & Bell, A. Molecular and Biochemical Characterization of a Plasmodium Falciparum Cyclophilin Containing a Cleavable Signal Sequence. *Eur. J. Biochem.* **232**, 765–772 (1995).

23. Mok, S. *et al.* Population transcriptomics of human malaria parasites reveals the mechanism of artemisinin resistance. *Science* **347**, 431–435 (2015).

24. Clark, A., Imperato, P. J. & Baker, K. M. Mali | Culture, History, & People. *Encyclopedia Britannica* (2020).

25. Malaria country profiles: Mali. (2017).

26. Malaria in Africa. *UNICEF DATA* https://data.unicef.org/topic/child-health/malaria/.

27. M, V. *et al.* Using CF11 cellulose columns to inexpensively and effectively remove human DNA from Plasmodium falciparum-infected whole blood samples. *Malar. J.* **11**, 41–41 (2012).

28. INV10-Standard-Operating-Procedure-Ring-Stage-Survival-Assays.pdf.

29. Lavstsen, T. *et al.* Plasmodium falciparum erythrocyte membrane protein 1 domain cassettes 8 and 13 are associated with severe malaria in children. *Proc. Natl. Acad. Sci. U. S. A.* **109**, E1791-1800 (2012).

30. Bauminger, E. R., Cohen, S. G., Ofer, S. & Rachmilewitz, E. A. Quantitative studies of ferritinlike iron in erythrocytes of thalassemia, sickle-cell anemia, and hemoglobin Hammersmith with Mossbauer spectroscopy. *Proc. Natl. Acad. Sci.* **76**, 939–943 (1979).

31. Chaves, M. A. F., Leonart, M. S. S. & do Nascimento, A. J. Oxidative process in erythrocytes of individuals with hemoglobin S. *Hematology* **13**, 187–192 (2008).

32. Percário, S. *et al.* Oxidative Stress in Malaria. *Int. J. Mol. Sci.* **13**, 16346–16372 (2012).

33. Clark, I. A. & Hunt, N. H. Evidence for reactive oxygen intermediates causing hemolysis and parasite death in malaria. *Infect. Immun.* **39**, 1–6 (1983).

34. Flick, K. & Chen, Q. var genes, PfEMP1 and the human host. *Mol. Biochem. Parasitol.* **134**, 3–9 (2004).

35. Pasternak, N. D. & Dzikowski, R. PfEMP1: an antigen that plays a key role in the pathogenicity and immune evasion of the malaria parasite Plasmodium falciparum. *Int. J. Biochem. Cell Biol.* **41**, 1463–1466 (2009).

36. White, N. J. *et al.* Malaria. *Lancet Lond. Engl.* **383**, 723–735 (2014).

37. Grüring, C. *et al.* Development and host cell modifications of Plasmodium falciparum blood stages in four dimensions. *Nat. Commun.* **2**, 165 (2011).

38. The Cinderella syndrome: why do malaria-infected cells burst at midnight? *Trends Parasitol.* **29**, 10–16 (2013).

39. Ciuffreda, L., Zoiku, F. K., Quashie, N. B. & Ranford-Cartwright, L. C. Estimation of parasite age and synchrony status in Plasmodium falciparum infections. *Sci. Rep.* **10**, (2020).

40. Marti, M., Good, R. T., Rug, M., Knuepfer, E. & Cowman, A. F. Targeting malaria virulence and remodeling proteins to the host erythrocyte. *Science* **306**, 1930–1933 (2004).